East Asian Journal on Applied Mathematics
doi: 10.4208/eajam.181016.300517g

Vol. 7, No. 4, pp. 697-713
November 2017

High Order Well-Balanced Weighted Compact Nonlinear Schemes for the Gas Dynamic Equations under Gravitational Fields

Zhen Gao[1] and Guanghui Hu[2,3]*

[1] *School of Mathematical Sciences, Ocean University of China, Qingdao, China.*
[2] *Department of Mathematics, University of Macau, Macao SAR, China*
[3] *UM Zhuhai Research Institute, Zhuhai, Guangdong Province, China.*

Received 18 October 2016; Accepted (in revised version) 30 May 2017.

Abstract. In this study, we propose a high order well-balanced weighted compact nonlinear (WCN) scheme for the gas dynamic equations under gravitational fields. The proposed scheme is an extension of the high order WCN schemes developed in (S. Zhang, S. Jiang, C.-W Shu, J. Comput. Phys. 227 (2008) 7294-7321). For the purpose of maintaining the exact steady state solution, the well-balanced technique in (Y. Xing, C.-W Shu, J. Sci. Comput. 54 (2013) 645-662) is employed to split the source term into two terms. The proposed scheme can maintain the isothermal equilibrium solution exactly, genuine high order accuracy and resolve small perturbations of the hydrostatic balance state on the coarse meshes. Furthermore, in order to capture the strong discontinuities and large gradients, the fifth-order upwind weighted nonlinear interpolations together with the fourth/sixth order cell-centered compact schemes with local characteristic projections are used to construct different WCN schemes. Several representative one- and two-dimensional examples are simulated to demonstrate the good performance of the proposed schemes.

AMS subject classifications: 35L65, 35L67

Key words: Euler equations, gravitational fields, source term, steady state solution, weighted compact nonlinear Scheme.

1. Introduction

Gas dynamic equations under gravitational fields are important in describing the astrophysical and atmospheric phenomena such as supernova explosions [14], and climate modeling and weather forecasting [4]. Since many astrophysical problems involving the hydrodynamical evolution in a gravitational field, correctly capturing the effect of gravitational force plays an important role in the long time simulations of star and galaxy formation. Failure on such capturing would lead to a solution which either oscillates around the equilibrium, or deviates from the equilibrium after a long time simulation.

*Corresponding author. *Email addresses:* zhengao@ouc.edu.cn (Z. Gao), garyhu@umac.mo (G. H. Hu)

 ©2017 Global-Science Press

https://doi.org/10.4208/eajam.181016.300517g Published online by Cambridge University Press

Therefore, a reliable numerical scheme for this problem should maintain the precise balance of pressure and gravitational forces in case of the hydrostatic solution. The well-balanced schemes can preserve exactly these steady state solutions up to machine accuracy. They are also specially designed to ensure accurate simulations and exhibit essential stability properties on relatively coarse meshes. In the last two decades, several well-balanced pioneering works have been designed. For example, LeVeque and Bale [16] extended the quasi-steady wave-propagation methods for the Euler equations under a static gravitational field. In [22, 31], Xu and his collaborators designed the well-balanced gas-kinetic scheme for multidimensional gas dynamic equations under gravitational field. The well-balanced Runge-Kutta discontinuous Galerkin method [18] and nodal discontinuous Galerkin method [6] for the Euler equations under gravitational fields can preserve the isothermal hydrostatic solution up to machine precision. A second-order well-balanced central-upwind scheme for the Euler equations of gas dynamics with gravitation was proposed in [7]. An approximate Riemann solver using the formalism of Harten, Lax and van Leer was developed to derive a well-balanced numerical scheme to obtain the solutions of the Euler equations with a gravitational potential in [11]. High order Weighted Essentially Non-Oscillation (WENO) finite difference well-balanced scheme for the isothermal equilibrium was introduced in [33]. High order well-balanced finite volume WENO schemes preserving not only the isothermal equilibrium but also the polytropic hydrostatic balance state exactly was proposed in [19]. Another popular hyperbolic balance laws with source terms in the literature is the shallow water equations over a non-flat bottom topology which also need the well-balanced methods to maintain a delicate balance of the divergence of the flux and the source terms in the steady state solution, such as [1,2,16,20,27,32,36,37,39] and the references therein.

Based on the idea of WENO scheme, a class of weighted compact nonlinear (WCN) schemes were developed [9, 10] which has better wave resolution and similar ability to capture discontinuities as the classical WENO scheme. Then it has been extended to the ninth order [23,26,38] which demonstrates the increasing resolutions with the increasing orders. The WCN schemes also show suitable freestream and vortex preservation properties on a wavy grid [25]. In order to preserve the positivity of both density and pressure in the complex flow problems with severe discontinuities, the robust WCN schemes were proposed in [8, 21, 24] respectively. The corresponding robust WCN scheme was successfully employed to simulate the hydrogen/air detonation [24]. Recently, the high order well-balanced WCN schemes for shallow water equations were designed in [12].

In this paper, a numerical framework of the high order well-balanced WCN schemes is designed for the one- and two-dimensional gas dynamic equations under gravitational fields. It is an extension of the high order WCN scheme [38] and well-balanced WENO scheme [33]. The proposed schemes can be proved that the isothermal equilibrium solution and genuine high order accuracy can be exactly maintained by rigorous theoretical analysis. In the numerical simulations, the first order global Lax-Friedrichs flux splitting is used to introduce correct upwinding and enhance the numerical stability. To reach the high order accuracy, the fifth-order upwind weighted nonlinear interpolations together with the fourth/sixth order cell-centered compact schemes are employed. To further restrain the

https://doi.org/10.4208/eajam.181016.300517g Published online by Cambridge University Press

numerical oscillations around the strong discontinuities and large gradients, the local characteristic projections on the conservative fluxes are also considered. Besides the high order numerical accuracy and the non-oscillatory behavior, the ability on well resolving small perturbations of the proposed schemes can also be observed successfully from the numerical experiments.

The paper is organized as follows. We begin in Section 2 with a brief review of the formulation of the high order WCN schemes. In Section 3, the high order well-balanced WCN schemes for the gas dynamic equations under gravitational fields is described in detail. In Section 4, several classical examples are presented to verify the high order accuracy, the well-balanced property and good resolution for smooth and discontinuous solutions. Conclusions are given in Section 5.

2. A Review of Weighted Compact Nonlinear Scheme

Consider a uniformly spaced grid defined by the points $x_i = i\Delta x$, $i = 0, \cdots, N$, which are called cell centers, with cell boundaries given by $x_{i+\frac{1}{2}} = x_i + \frac{\Delta x}{2}$, where Δx is the uniform grid spacing. The semi-discretized form of the gas dynamic equations (See Eq. (3.1)) without source terms is transformed into the system of ordinary differential equations and solved by the method of lines

$$\frac{du_i(t)}{dt} = -f_i^{'}, \quad i = 0, \cdots, N, \tag{2.1}$$

where $f_i^{'}$ is the numerical approximation to the spatial derivative at the cell centers x_i.

2.1. Cell-centered compact scheme

Given the function values on a set of nodes, a linear cell-centered compact scheme [15] approximation to $f_i^{'}$ is expressed as

$$\beta f_{i-2}^{'} + \alpha f_{i-1}^{'} + f_i^{'} + \alpha f_{i+1}^{'} + \beta f_{i+2}^{'} = c\frac{f_{i+\frac{5}{2}} - f_{i-\frac{5}{2}}}{5\Delta x} + b\frac{f_{i+\frac{3}{2}} - f_{i-\frac{3}{2}}}{3\Delta x} + a\frac{f_{i+\frac{1}{2}} - f_{i-\frac{1}{2}}}{\Delta x}. \tag{2.2}$$

If $\beta = 0$, $c = 0$, a fourth ($\alpha = 1/22$) or sixth ($\alpha = 9/62$) order tridiagonal compact scheme can be obtained with $a = (3-2\alpha)3/8$ and $b = (22\alpha - 1)/8$. The derivatives at the two boundary points f_0' and f_N' are computed by the fifth order WENO-Z scheme [3, 5].

2.2. Weighted nonlinear interpolation

Here, we briefly review the basic idea of the high order weighted nonlinear interpolation and take fifth order ($r = 3$) interpolation for example. Similar to the idea of WENO reconstruction, the key issue of the weighted interpolation is the following polynomial reconstruction procedure. The 5-point ($2r - 1 = 5$) global stencil $S^5 = (x_{i-2}, \cdots, x_{i+2})$ is subdivided into three 3-point substencils $S_k = (x_{i+k-2}, x_{i+k-1}, x_{i+k}), (k = 0, 1, 2)$. The fifth

https://doi.org/10.4208/eajam.181016.300517g Published online by Cambridge University Press

degree polynomial approximation $\hat{f}_{i+\frac{1}{2}} = \tilde{f}(f_{i-2}, \cdots, f_{i+2})$ is built through the convex combination of three second order interpolation polynomials $\hat{f}^k(x)$ in substencils S_k at the cell boundaries $x_{i+\frac{1}{2}}$,

$$\begin{aligned}\hat{f}_{i+\frac{1}{2}} =& \frac{1}{128}(3f_{i-2} - 20f_{i-1} + 90f_i + 60f_{i+1} - 5f_{i+2}),\\ =& \sum_{k=0}^{2} d_k \hat{f}^k(x_{i+\frac{1}{2}}),\end{aligned} \tag{2.3}$$

where $(d_0, d_1, d_2) = (1/16, 10/16, 5/16)$ are the linear weights and

$$\begin{aligned}\hat{f}^0(x_{i+\frac{1}{2}}) &= \frac{1}{8}(3f_{i-2} - 10f_{i-1} + 15f_i),\\ \hat{f}^1(x_{i+\frac{1}{2}}) &= \frac{1}{8}(-f_{i-1} + 6f_i + 3f_{i+1}),\\ \hat{f}^2(x_{i+\frac{1}{2}}) &= \frac{1}{8}(3f_i + 6f_{i+1} - f_{i+2}).\end{aligned} \tag{2.4}$$

To capture the discontinuities and large gradients without spurious oscillation, the idea of normalized nonlinear weights ω_k in the WENO reconstruction is used to replace the linear weights d_k. And then we can obtain the weighted interpolation approximation [38] as

$$\hat{f}_{i+\frac{1}{2}} = \sum_{k=0}^{2} \omega_k \hat{f}^k(x_{i+\frac{1}{2}}), \tag{2.5}$$

where

$$\omega_k = \frac{\alpha_k}{\sum_{j=0}^{2} \alpha_j}, \quad \alpha_k = \frac{d_k}{(\beta_k + \varepsilon)^p}, \quad k = 0, 1, 2. \tag{2.6}$$

Here, the sensitivity parameter $\varepsilon > 0$ is a small number to avoid divisions by zero. The power parameter $p \geq 1$ is used to enhance the relative ratio between the smoothness indicators β_k which is defined by

$$\beta_k = \sum_{l=1}^{2} \Delta x^{2l-1} \int_{x_{i-\frac{1}{2}}}^{x_{i+\frac{1}{2}}} \left(\frac{d^l}{dx^l} \hat{f}^k(x) \right)^2 dx, \quad k = 0, 1, 2. \tag{2.7}$$

The explicit expressions for the smoothness indicators β_k can be found in [13, 38]. The weighted formulation Eq. (2.6) in the classical reconstruction procedure of the WENO scheme [13] is too dissipative and lose the accuracy at the critical points. An improved nonlinear weights [3, 5] are defined as

$$\alpha_k = d_k \left(1 + \left(\frac{\tau_5}{\beta_k + \epsilon} \right)^p \right), \quad \omega_k = \frac{\alpha_k}{\sum_{l=0}^{2} \alpha_l}, \quad k = 0, 1, 2, \tag{2.8}$$

where $\tau_5 = |\beta_2 - \beta_0|$. $\varepsilon = 10^{-12}$ and $p = 2$ are used in this study.

https://doi.org/10.4208/eajam.181016.300517g Published online by Cambridge University Press

The upwinding flux splitting technique is used to enhance the numerical stability

$$f(Q) = f^{+}(Q) + f^{-}(Q), \tag{2.9}$$

where $df^{+}(Q)/dQ \geq 0$ and $df^{+}(Q)/dQ \leq 0$. One example is a simple global Lax-Friedrichs flux splitting

$$f^{\pm}(Q) = \frac{1}{2}(f(Q) \pm \alpha Q), \tag{2.10}$$

where $\alpha = \max_i |\lambda_i(Q)|$ with $\lambda_i(Q)$ being the i-th eigenvalue of the Jacobian matrix $f^{'}(Q)$, and $f^{\pm}(Q)$ are positive and negative fluxes respectively.

The fourth and sixth order centered compact schemes combine with the fifth order weighted interpolation result in the fourth and fifth order WCN schemes respectively. We refer to [38] for generalized formulations of the higher order WCN schemes.

3. Well-Balanced Weighted Compact Nonlinear Scheme

The gas dynamic equations, coupled with a static gravitational potential can be written compactly as

$$Q_t + \nabla \cdot F(Q) = S, \tag{3.1}$$

where Q, $F(Q)$ and S are vectors of the conservative variables, flux and source terms respectively. In the one-dimensional case, Eq. (3.1) has a specific form with

$$Q = \begin{bmatrix} \rho \\ \rho u \\ E \end{bmatrix}, \qquad F = \begin{bmatrix} \rho u \\ \rho u^2 + P \\ (E+P)u \end{bmatrix}, \qquad S = \begin{bmatrix} 0 \\ -\rho \phi_x \\ -\rho u \phi_x \end{bmatrix}. \tag{3.2}$$

Here ρ is density, P is pressure and u is the velocity. The non-gravitational energy E is given by,

$$E = \frac{P}{\gamma - 1} + \frac{1}{2}\rho u^2, \tag{3.3}$$

where γ is the ratio of ideal gas. $\phi = \phi(x)$ is the time independent gravitational potential.

For the static gravitational potential $\phi(x)$, Eq. (3.1) admits a special steady state solution,

$$\rho = \rho(x), \qquad u = 0, \qquad P_x = -\rho \phi_x, \tag{3.4}$$

with a constant temperature and zero velocity. For an ideal gas, we have the relation

$$P = \rho RT, \tag{3.5}$$

where R is the gas constant, and T is the temperature. Combined with the steady state equation $P_x = -\rho \phi_x$ from Eq. (3.1), it becomes

$$\rho(x) = \rho_0 \exp\left(-\frac{\phi}{RT}\right), \tag{3.6}$$

https://doi.org/10.4208/eajam.181016.300517g Published online by Cambridge University Press

which leads to the special steady state

$$\rho = \rho_0 \exp\left(-\frac{\phi}{RT}\right), \quad u = 0, \quad P = RT\rho_0 \exp\left(-\frac{\phi}{RT}\right), \tag{3.7}$$

with constant temperature T. If the linear gravitational potential field: $\phi_x = g$ is considered, we can obtain the simplest and most commonly encountered hydrostatic balance

$$\rho = \rho_0 \exp(-g\rho_0 x/P_0), \quad u = 0, \quad P = P_0 \exp(-g\rho_0 x/P_0). \tag{3.8}$$

A special steady state of Eq. (3.8) is given by

$$\rho = c(-gx), \quad u = 0, \quad P = c\exp(-gx). \tag{3.9}$$

We start from Eq. (3.9) to introduce the well-balanced WCN scheme for the one-dimensional gas dynamic equations under gravitational fields. Borrowed the idea from [33], the source term S in Eq. (3.2) is reformulated into two terms as

$$S = \left(0, \ \rho\exp(gx)(\exp(-gx))_x, \ \rho u\exp(gx)(\exp(-gx))_x\right)^{T_s}, \tag{3.10}$$

where T_s is the transpose operator. And then each derivative is independently discretized by using the same nonlinear weights as those computed from approximating the flux derivative terms in the conservation laws. Similar procedure has been used in the high order well-balanced WENO method for the shallow-water equations [34] and a class of hyperbolic systems with source terms [35].

In this work, the conservative variables $Q = (\rho, \rho u, E)$ in Eq. (2.10) is replaced by $Q^* = (\rho\exp(gx), \rho u\exp(gx), E\exp(gx))$. The same technique is used in the literature [33]. The flux $F(Q)$ is split up into

$$F(Q) = F^+(Q) + F^-(Q), \tag{3.11}$$

where

$$F^{\pm}(Q) = \frac{1}{2}\left[\begin{pmatrix} \rho u \\ \rho u^2 + P \\ (E+P)u \end{pmatrix} \pm \alpha_0 \begin{pmatrix} \rho\exp(gx) \\ \rho u\exp(gx) \\ E\exp(gx) \end{pmatrix}\right], \tag{3.12}$$

where $\alpha_0 = \alpha \max_x \exp(-gx)$. See [13, 28] for more details. Moreover, the derivatives in the source terms are also split up into their positive and negative parts as

$$\begin{pmatrix} 0 \\ \exp(-gx) \\ \exp(-gx) \end{pmatrix}_x = \frac{1}{2}\begin{pmatrix} 0 \\ \exp(-gx) \\ \exp(-gx) \end{pmatrix}_x^+ + \frac{1}{2}\begin{pmatrix} 0 \\ \exp(-gx) \\ \exp(-gx) \end{pmatrix}_x^-. \tag{3.13}$$

Proposition 3.1. *Weighted compact nonlinear schemes with a linear interpolation Eq.* (2.3) *for the gas dynamic equations with the linear gravitational potential field Eq.* (3.1) *satisfying the steady state solution Eq.* (3.9) *can preserve the steady state solution exactly.*

https://doi.org/10.4208/eajam.181016.300517g Published online by Cambridge University Press

Proof. Firstly, $\hat{F}^+_{j+\frac{1}{2}}$ has the following expression,

$$\begin{aligned}\hat{F}^+_{j+\frac{1}{2}} &= \sum_{k=-2}^{2} d_k F^+_{j+k} \\ &= \sum_{k=-2}^{2} d_k \frac{1}{2}(F_{j+k} + \alpha_0 Q^*_{j+k}) \\ &= \frac{1}{2}\sum_{k=-2}^{2} d_k F_{j+k} + \frac{1}{2}\sum_{k=-2}^{2} d_k(\alpha_0 Q^*_{j+k}).\end{aligned} \tag{3.14}$$

Similarly, $\hat{F}^-_{j+\frac{1}{2}}$ can be expressed as

$$\hat{F}^-_{j+\frac{1}{2}} = \frac{1}{2}\sum_{k=-1}^{3} e_k F_{j+k} - \frac{1}{2}\sum_{k=-1}^{3} e_k(\alpha_0 Q^*_{j+k}). \tag{3.15}$$

Since Q^* is a constant vector and $\sum_{k=-2}^{2} d_k = \sum_{k=-1}^{3} e_k = 1$,

$$\begin{aligned}\sum_{k=-2}^{2} d_k(\alpha_0 Q^*_{j+k}) &= \alpha_0(c, 0, c/(\gamma-1))^{T_s}, \\ \sum_{k=-1}^{3} e_k(\alpha_0 Q^*_{j+k}) &= \alpha_0(c, 0, c/(\gamma-1))^{T_s},\end{aligned} \tag{3.16}$$

then

$$\begin{aligned}\hat{F}_{j+\frac{1}{2}} &= \hat{F}^+_{j+\frac{1}{2}} + \hat{F}^-_{j+\frac{1}{2}} \\ &= \frac{1}{2}\sum_{k=-2}^{2} d_k F_{j+k} + \frac{1}{2}\sum_{k=-1}^{3} e_k F_{j+k}.\end{aligned} \tag{3.17}$$

We take the fourth order compact scheme Eq. (2.2) for example. The right hand side is

$$a\frac{\hat{F}_{j+\frac{1}{2}} - \hat{F}_{j-\frac{1}{2}}}{\Delta x} = \frac{a}{2\Delta x}\left(\sum_{k=-2}^{2} d_k F_{j+k} + \sum_{k=-1}^{3} e_k F_{j+k}\right) - \frac{a}{2\Delta x}\left(\sum_{k=-3}^{1} f_k F_{j+k} + \sum_{k=-2}^{2} d_k F_{j+k}\right). \tag{3.18}$$

The steady state solution Eq. (3.9) is used and the corresponding source term becomes $S = (0, c(\exp(-gx))_x, 0)^T = (0, P_x, 0)^T$. By using the same procedure above to the source term **S** of Eq. (3.2), we can obtain

$$a\frac{\hat{S}_{j+\frac{1}{2}} - \hat{S}_{j-\frac{1}{2}}}{\Delta x} = \frac{a}{2\Delta x}\left(\sum_{k=-2}^{2} d_k S_{j+k} + \sum_{k=-1}^{3} e_k S_{j+k}\right) - \frac{a}{2\Delta x}\left(\sum_{k=-3}^{1} f_k S_{j+k} + \sum_{k=-2}^{2} d_k S_{j+k}\right). \tag{3.19}$$

https://doi.org/10.4208/eajam.181016.300517g Published online by Cambridge University Press

Therefore, the first and third components of Eq. (3.18) and Eq. (3.19) are equal to zeros. The second component of Eq. (3.18) becomes

$$a\frac{\hat{P}_{j+\frac{1}{2}}-\hat{P}_{j-\frac{1}{2}}}{\Delta x}=\frac{a}{2\Delta x}\left(\sum_{k=-2}^{2}d_kP_{j+k}+\sum_{k=-1}^{3}e_kP_{j+k}\right)-\frac{a}{2\Delta x}\left(\sum_{k=-3}^{1}f_kP_{j+k}+\sum_{k=-2}^{2}d_kP_{j+k}\right). \tag{3.20}$$

The second component of Eq. (3.19) is equal to Eq. (3.20). Hence,

$$a\frac{\hat{F}_{j+\frac{1}{2}}-\hat{F}_{j-\frac{1}{2}}}{\Delta x}-a\frac{\hat{S}_{j+\frac{1}{2}}-\hat{S}_{j-\frac{1}{2}}}{\Delta x}=0. \tag{3.21}$$

Therefore, the steady state solution Eq. (3.9) can be preserved exactly. By similar procedure, the extension to other higher order WCN schemes is straightforward. This finishes the proof. □

However, the high order WCN schemes described in the Section 2 are nonlinear. The nonlinearity comes from the nonlinear weights, which in turn comes from the nonlinearity of the smooth indicators β_k measuring the regularity of the fluxes F^+ and F^-. To maintain the steady state solution exactly and high order accuracy, we use the same nonlinear weights as computed from two terms $(\rho u^2+P)_x$ and $((E+P)u)_x$ to $(\exp(-gx))_x$. Therefore, the nonlinear interpolation formulation Eq. (2.5) becomes a linear interpolation formulation and satisfy the proposition (3.1).

In case of the WCN schemes with local characteristic decomposition, we do the same local characteristic decomposition to two terms in Eq. (3.24) by using the local characteristic matrix of Eq. (3.12). The nonlinear interpolation weights computed from the characteristic variables are used to the corresponding variables of Eq. (3.24) after the characteristic projection. We can prove that the WCN schemes with local characteristic decomposition and flux splitting Eq. (3.12), and with the special handling of the source terms described above, maintains exactly the steady state solution.

Next, we design the high order well-balanced WCN scheme for the general steady state Eq. (3.7). The source term in Eq. (3.2) is reformulated as

$$S=\begin{bmatrix}0\\ RT\rho\exp\left(\frac{\phi}{RT}\right)\left(\exp\left(-\frac{\phi}{RT}\right)\right)_x\\ RT\rho u\exp\left(\frac{\phi}{RT}\right)\left(\exp\left(-\frac{\phi}{RT}\right)\right)_x\end{bmatrix}. \tag{3.22}$$

The corresponding flux splitting and the derivatives in the source terms are replaced by

$$F^{\pm}(Q)=\frac{1}{2}\left[\begin{pmatrix}\rho u\\ \rho u^2+P\\ (E+P)u\end{pmatrix}\pm\alpha_0\begin{pmatrix}\rho\exp(\frac{\phi}{RT})\\ \rho u\exp(\frac{\phi}{RT})\\ E\exp(\frac{\phi}{RT})\end{pmatrix}\right], \tag{3.23}$$

and

$$\begin{pmatrix}0\\ \exp(-\frac{\phi}{RT})\\ \exp(-\frac{\phi}{RT})\end{pmatrix}_x=\frac{1}{2}\begin{pmatrix}0\\ \exp(-\frac{\phi}{RT})\\ \exp(-\frac{\phi}{RT})\end{pmatrix}^+_x+\frac{1}{2}\begin{pmatrix}0\\ \exp(-\frac{\phi}{RT})\\ \exp(-\frac{\phi}{RT})\end{pmatrix}^-_x. \tag{3.24}$$

https://doi.org/10.4208/eajam.181016.300517g Published online by Cambridge University Press

Finally, we extend the high order well-balanced WCN schemes into the two-dimensional gas dynamic equations under a gravitational field Eq. (3.1) with

$$Q=\begin{bmatrix}\rho\\ \rho u\\ \rho v\\ E\end{bmatrix},\quad F=\begin{bmatrix}\rho u\\ \rho uv\\ \rho u^2+P\\ (E+P)u\end{bmatrix},\quad G=\begin{bmatrix}\rho v\\ \rho v^2+P\\ \rho uv\\ (E+P)v\end{bmatrix},\quad S=\begin{bmatrix}0\\ -\rho\phi_x\\ -\rho\phi_y\\ -\rho u\phi_x-\rho v\phi_y\end{bmatrix}, \tag{3.25}$$

where (u,v) is the velocity vector and ρ, P, $\phi(x,y)$ follow the definitions below Eq. (3.2). $E=\frac{P}{\gamma-1}+\frac{1}{2}\rho(u^2+v^2)$ is the non-gravitational energy. With the constant temperature and zero velocity, the hydrostatic balance of Eq. (3.1) is the steady state solution

$$\rho=\rho_0\exp\left(-\frac{\phi}{RT}\right),\quad u=v=0,\quad P=RT\rho_0\exp\left(-\frac{\phi}{RT}\right), \tag{3.26}$$

and the steady state solution corresponding to the linear gravitational potential field: $\phi_x=g_1$ and $\phi_y=g_2$ takes the form

$$\rho=\rho_0\exp\left(\frac{-\rho_0(g_1x+g_2y)}{P_0}\right),\quad u=v=0,\quad P=P_0\exp\left(\frac{-\rho_0(g_1x+g_2y)}{P_0}\right). \tag{3.27}$$

For preserving the steady state solution Eq. (3.26), we modify the source term as

$$S=\begin{bmatrix}0\\ RT\rho\exp\left(\frac{\phi}{RT}\right)\left(\exp\left(-\frac{\phi}{RT}\right)\right)_x\\ RT\rho\exp\left(\frac{\phi}{RT}\right)\left(\exp\left(-\frac{\phi}{RT}\right)\right)_y\\ RT\rho u\exp\left(\frac{\phi}{RT}\right)\left(\exp\left(-\frac{\phi}{RT}\right)\right)_x+RT\rho v\exp\left(\frac{\phi}{RT}\right)\left(\exp\left(-\frac{\phi}{RT}\right)\right)_y\end{bmatrix}, \tag{3.28}$$

and use the one-dimensional procedure described above in the x- and y-directions respectively. Therefore, the high order accuracy and the exact steady state solution can be maintained.

The resulting system of ordinary differential equations after spatial discretization is advanced in time via the third order TVD Runge-Kutta scheme [29]. The CFL condition is set to be CFL = 0.45 in the numerical experiments performed in this study.

4. Numerical Results

In this section, several classical one- and two-dimensional examples taken from [17, 22, 31, 33] will be illustrated to show the behaviors of the well-balanced WCN scheme preserving the hydrostatic balance state, meanwhile maintaining the genuine high order accuracy and the capability of computation on the small perturbation of a steady state solution on a relatively coarse mesh. Since the corresponding results of ρv are similar to those of ρu in the two-dimensional cases, they are omitted here. For clarity, the fourth and sixth order compact schemes coupled with the fifth order nonlinear interpolation method are named as the WCN4 scheme and WCN6 scheme respectively. We shall collectively refer to the WCN4 and WCN6 schemes as the WCN schemes.

https://doi.org/10.4208/eajam.181016.300517g Published online by Cambridge University Press

Table 1: L_∞ errors for ρ, ρu and E as computed by the WCN schemes at time $t=2$.

N	40			200		
L_∞	ρ	ρu	E	ρ	ρu	E
WCN4	7.8E-16	5.2E-16	1.1E-15	3.0E-15	7.7E-16	1.6E-15
WCN6	1.1E-15	3.4E-16	1.6E-15	3.7E-15	7.5E-16	1.8E-15

4.1. One-dimensional isothermal equilibrium solution

We consider the one-dimensional isothermal equilibrium solution in the form of Eq. (3.9) which is given by

$$\rho_0(x)=\exp(-x),\quad u_0(x)=0,\quad P_0(x)=\exp(-x), \tag{4.1}$$

with $\gamma=1.4$ and the linear gravitational field $\phi_x=g=1$. The computational domain is set as $[0,1]$.

The steady state solution Eq. (4.1), which should be exactly preserved, is used as the initial condition to show the well-balanced property of the WCN schemes. We use double precision to perform the computation until the final time $t=2$. The L_∞ errors of the difference for ρ, ρu and E between the initial condition and the final solution computed by the WCN schemes with $N=40$ and 200 uniform cells are shown in Table 1. Obviously, the L_∞ errors are at the level of round-off errors for different resolutions, which verify the well-balanced property of the WCN schemes.

Next, we impose a small perturbation to the initial pressure state

$$P(x,t=0)=P_0(x)+\eta\exp\left(-100(x-0.5)^2\right), \tag{4.2}$$

where η is a non-zero perturbation constant ($\eta=0.01$ and $\eta=0.0001$ are used). The final time is $t=0.25$. The initial perturbation (the dashed lines in Fig. 1) will break into two smaller waves propagating to the left and right directions respectively. The solutions computed by the WCN schemes with $N=200$ grid points are drawn in Fig. 1 which are in a good agreement with reference solution (computed by the WCN6 scheme with $N=2000$ grid points) and those in [17,22,31,33]. We can find that the proposed schemes accurately captures both small and large perturbations on a relatively coarse mesh with $N=200$.

4.2. Shock tube under gravitational field

The next example is the standard Sod tube test under gravitational field ϕ with a value of $g=\phi_x=1$ [22,33]. We assume the computational domain to be $[0,1]$ and the initial condition is

$$(\rho,u,P)=\begin{cases} (\ 0.125,\ 0.000,\ 0.1000\ ), & x\geq 0.5,\\ (\ 1.000,\ 0.000,\ 1.0000\ ), & x\leq 0.5.\end{cases}$$

The reflective boundary conditions are imposed on both ends of the domain. The final time is $t=0.2$. The number of uniform cells is $N=100$. Since there is no exact solution

https://doi.org/10.4208/eajam.181016.300517g Published online by Cambridge University Press

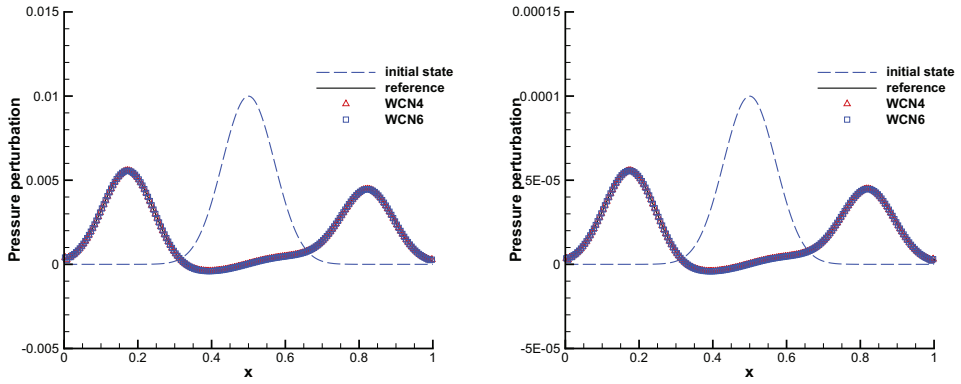


Figure 1: One-dimensional isothermal equilibrium solution with a small perturbation Eq. (4.2). The pressure perturbation with (Left) $\eta = 0.01$ and (Right) $\eta = 0.0001$ of the hydrostatic solution are computed by the WCN schemes at time $t = 0.25$.

for this problem, the numerical solution computed by the WCN6 scheme with $N = 2000$ grid points is used as the reference solution. We show the density, velocity, energy and pressure computed by the WCN schemes with $N = 100$ grid points in Fig. 2 which agree well the reference solution and those in [22,33]. Due to the gravitational force, the density distribution inside the tube is pulling towards the left direction, and negative velocity is found in the intervals $[0, 0.3]$ and $[0.85, 0.9]$ respectively. As one can see, the WCN schemes capture the solutions on the relatively coarse mesh of 100 grid points quite well.

4.3. One-dimensional gas falling into a fixed external potential

The same gas dynamic equations with a static gravitational potential Eq. (3.2) and a constant temperature and zero velocity steady state solution Eq. (3.7) is considered with the parameters $\rho_0 = 1$, $R = 1$, $T = 0.6866$. The ratio of the specific heat has a value $\gamma = 5/3$. The gravitational potential has the form of a sine wave

$$\phi(x) = -\phi_0 \frac{L}{2\pi} \sin \frac{2\pi x}{L}, \tag{4.3}$$

where $L = 64$ is the computational domain length and $\phi_0 = 0.02$ is the amplitude. The computational domain is set to be $[0, 64]$. The periodic boundary conditions are implemented in this example.

Starting with the steady state Eq. (3.7) as the initial condition, the solution is updated to a time $t = 50$. Theoretically, the steady state should be maintained up to machine zeros. Table 2 demonstrates the L_∞ errors of the ρ, ρu and E computed by the WCN schemes on different mesh sizes $N = 40$ and 200 respectively. In all cases we find that the L_∞ errors are small and of the order of machine precision.

Next, a small pressure perturbation added into the steady state Eq. (3.7) is used as the

https://doi.org/10.4208/eajam.181016.300517g Published online by Cambridge University Press

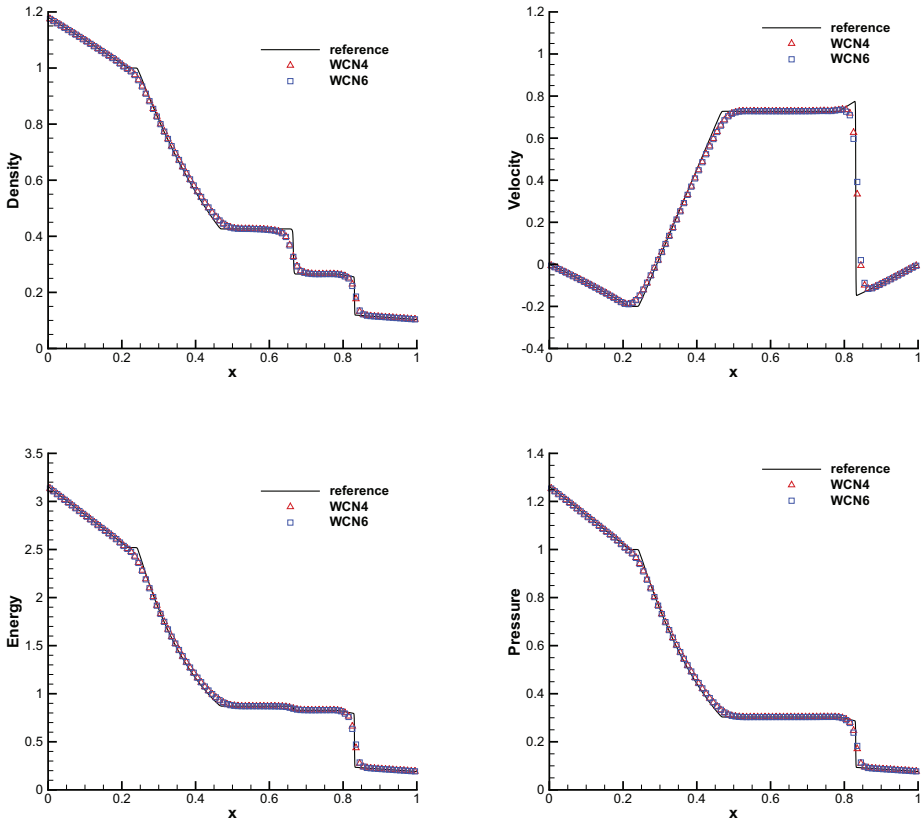


Figure 2: One-dimensional shock tube problem under gravitational field. The physical variables (Top left) density, (Top right) velocity, (Bottom left) energy and (Bottom right) pressure are computed by the WCN schemes at time $t = 0.2$.

Table 2: L_∞ errors for ρ, ρu and E as computed by the WCN schemes at time $t = 2$.

N	40			200		
L_∞	ρ	ρu	E	ρ	ρu	E
WCN4	1.1E-15	9.7E-16	1.1E-15	2.9E-15	1.1E-15	1.8E-15
WCN6	1.3E-15	7.9E-16	1.0E-15	2.7E-15	1.1E-15	2.0E-15

initial condition, such as,

$$\rho = \rho_0 \exp\left(-\frac{\phi}{RT}\right), \quad u = 0, \quad P = RT\rho_0 \exp\left(-\frac{\phi}{RT}\right) + 0.001\exp\left(-10(x-32)^2\right).$$

The system is expected to reach an isothermal hydrostatic state after long time simulation, where the temperature settles to a constant and fluid velocity is zero. Following the final time in [22], we compute the solution by the WCN schemes using $N = 64$ uniformly spaced grid points until the time $t = 2500000$ (5942976 time steps in our computation) and plot

https://doi.org/10.4208/eajam.181016.300517g Published online by Cambridge University Press

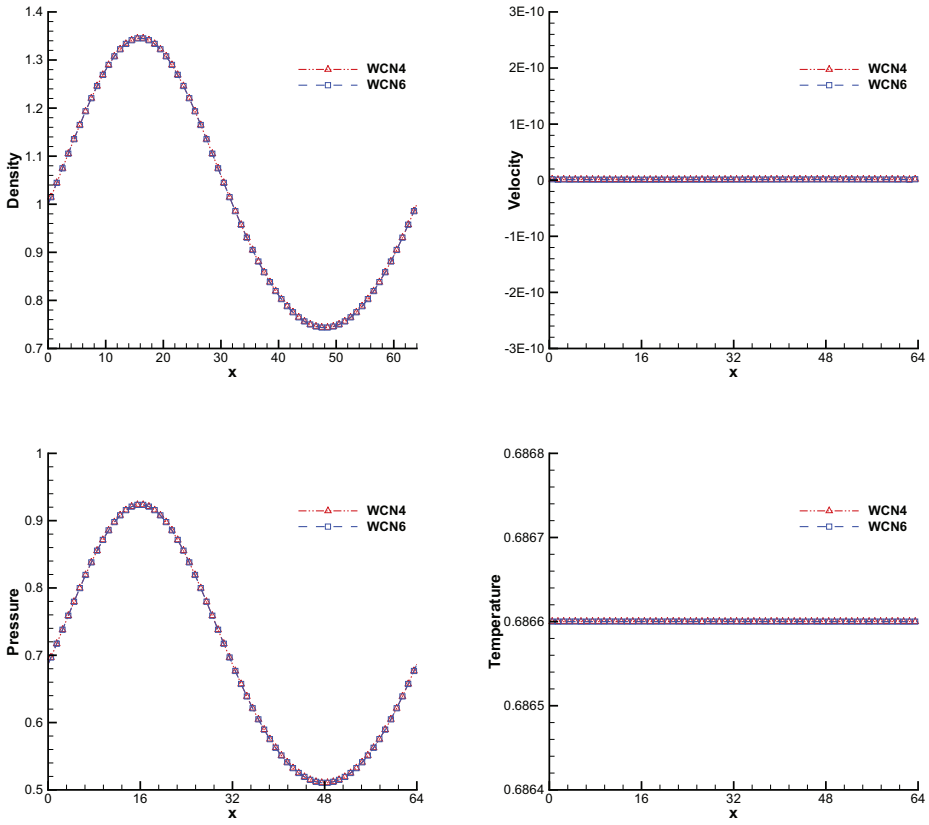


Figure 3: One-dimensional gas falling into a fixed external potential with a small perturbation Eq. (4.3). The physical variables (Top left) density, (Top right) velocity, (Bottom left) pressure and (Bottom right) temperature are computed by the WCN schemes at time $t = 2500000$.

the numerical results in Fig. 3. It can be clearly found that the results reach an isothermal hydrostatic state and are comparable to those in [22,30,31,33].

4.4. Order of accuracy for the two-dimensional case

The two-dimensional gas dynamic equations Eq. (3.25) with a linear gravitational field $\phi_x = \phi_y = 1$ will give an exact solution as

$$\rho(x,y,t) = 1 + 0.2\sin\big(\pi(x+y-t(u_0+v_0))\big), \quad u(x,y,t) = u_0, \quad v(x,y,t) = v_0,$$
$$P(x,y,t) = P_0 + t(u_0+v_0) - x - y + 0.2\cos\big(\pi(x+y-t(u_0+v_0))\big)/\pi,$$

with $u_0 = v_0 = 1$ and P_0=4.5. The computational domain is $[0,2]\times[0,2]$. The final time is $t = 0.1$. The exact solutions are used as the boundary condition. The time step Δt is taken to be proportional to $(1/\Delta x + 1/\Delta y)^{-4/3}$ and $(1/\Delta x + 1/\Delta y)^{-5/3}$ for the WCN4 and WCN6 schemes respectively. The L_∞ errors for ρ, ρu, E and numerical orders of accuracy

https://doi.org/10.4208/eajam.181016.300517g Published online by Cambridge University Press

Table 3: The accuracy test. L_∞ errors and numerical orders of accuracy for the WCN schemes.

Method	$N \times M$	ρ		ρu		E	
		error	order	error	order	error	order
WCN4	8×8	3.17E-2		3.19E-2		8.04E-3	
	16×16	5.39E-3	2.56	5.26E-3	2.60	3.33E-3	1.27
	32×32	4.35E-4	3.63	4.31E-4	3.61	1.25E-4	4.74
	64×64	2.36E-5	4.20	2.35E-5	4.20	2.34E-6	5.74
	128×128	7.55E-7	5.00	7.55E-7	4.96	6.73E-8	5.12
WCN6	8×8	3.26E-2		3.24E-2		1.08E-2	
	16×16	5.36E-3	2.60	5.22E-3	2.63	3.57E-3	1.60
	32×32	4.43E-4	3.60	4.39E-4	3.57	1.25E-4	4.84
	64×64	2.42E-5	4.19	2.41E-5	4.19	2.37E-6	5.72
	128×128	7.50E-7	5.01	7.50E-7	5.01	4.53E-8	5.71

for the WCN schemes are listed in Table 3. The fifth order of accuracy for the WCN4 and WCN6 schemes are observed. It is surprising that the numerical convergence order of the WCN4 scheme is one more than the expected fourth order.

4.5. Two-dimensional isothermal equilibrium solution

The isothermal equilibrium state with the linear gravitational field $\phi_x = \phi_y = g$ takes the form of

$$\rho(x,y) = \rho_0 \exp\left(-\frac{\rho_0 g}{P_0}(x+y)\right), \quad u(x,y) = u_0, \quad v(x,y) = v_0,$$
$$P(x,y) = P_0 \exp\left(-\frac{\rho_0 g}{P_0}(x+y)\right), \tag{4.4}$$

with the parameters $\gamma = 1.4$, $\rho_0 = 1.21$, $P_0 = 1$, $g = 1$ and $u_0 = v_0 = 0$. The computational domain is $[0,1] \times [0,1]$.

With the initial conditions Eq. (4.4), the numerical solutions computed by the WCN schemes using the double precision until the time $t = 1$ with 50×50 and 200×200 uniform grid points are shown in Table 4. One can clearly see that all the cases maintain the isothermal equilibrium state solution up to machine precision.

Next, we consider a small perturbation added into the initial pressure state of Eq. (4.4)

$$P(x,y) = P_0 \exp\left(-\frac{\rho_0 g}{P_0}(x+y)\right) + \eta \exp\left(-\frac{100\rho_0 g}{P_0}\left((x-0.3)^2 + (y-0.3)^2\right)\right), \tag{4.5}$$

to demonstrate the capability of the WCN schemes for the small perturbation to the stationary state. The simulation time is $t = 0.15$. We perform the computation with $N \times M = 50 \times 50$ and plot the results in Fig. 4 which agree well with the reference solution computed by the WCN6 scheme with $N \times M = 200 \times 200$ and those in [33]. It can be obviously observed that the WCN schemes are able to capture the small perturbation on the coarse mesh.

https://doi.org/10.4208/eajam.181016.300517g Published online by Cambridge University Press

Table 4: L_∞ errors for ρ, ρu and E as computed by the WCN schemes at time $t = 1$.

N	50×50			200×200		
L_∞	ρ	ρu	E	ρ	ρu	E
WCN4	2.0E-16	9.2E-17	2.0E-16	3.8E-16	1.3E-16	2.4E-16
WCN6	2.1E-16	8.5E-17	2.1E-16	3.9E-16	1.3E-16	2.4E-16

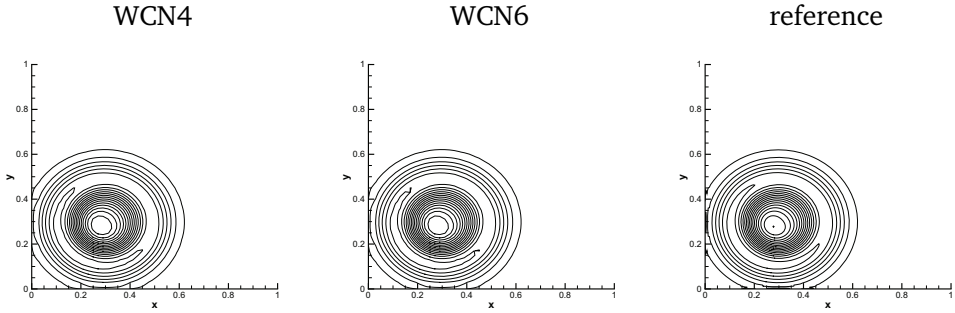


Figure 4: Two-dimensional isothermal equilibrium solution with a small perturbation Eq. (4.5). The contour lines of the pressure perturbation are computed by (Left) the WCN4 scheme and (Middle) the WCN6 scheme and (Right) the reference solution at time $t = 0.15$.

5. Concluding Remarks

In this work, we design the high order well-balanced weighted compact nonlinear (WCN) schemes for the gas dynamic equations under gravitational fields by reformulating the source term into two terms. The first order global Lax-Friedrichs flux splitting and local characteristic projections on the conservative fluxes are used to enhance the numerical stability. Extensive one- and two-dimensional examples are conducted to show that the proposed WCN schemes can exactly maintain the isothermal equilibrium solution, genuine high order accuracy and capture the small perturbations on the relative coarse grids.

Acknowlegements

The authors would like to acknowledge the funding support of this research by National Science and Technology Major Project (20101010), Shandong Provincial Natural Science Foundation (ZR2017MA016), National Natural Science Foundation of China (41306002), and Fundamental Research Funds for the Central Universities (201562012, 201564019). The first author gratefully acknowledges the invitation of Dr. Guanghui Hu and also extends his gratitude to the Faculty of Science and Technology at University of Macau for hosting his visit. The work of G. H. Hu was partially supported by 050/2014/A1 from FDCT of Macao S.A.R., MYRG2014-00109-FST from University of Macau, and National Natural Science Foundation of China (11401608).

https://doi.org/10.4208/eajam.181016.300517g Published online by Cambridge University Press

References

[1] E. Audusse, F. Bouchut, M.-O. Bristeau, R. Klein and B. Perthame, A fast and stable well-balanced scheme with hydrostatic reconstruction for shallow water flows, SIAM J. Sci. Comput. 25 (2004) 2050–2065.

[2] A. Bermudez and M.E. Vazquez, Upwind methods for hyperbolic conservation laws with source terms, Comput. Fluids. 23 (1994) 1049–1071.

[3] R. Borges, M. Carmona, B. Costa and W.S. Don, An improved weighted essentially non-oscillatory scheme for hyperbolic conservation laws, J. Comput. Phys. 227 (2008) 3101–3211.

[4] N. Botta, R. Klein, S. Langenberg and S. Lützenkirchen, Well-balanced finite volume methods for nearly hydrostatic flows, J. Comput. Phys. 196 (2004) 539–565.

[5] M. Castro, B. Costa and W.S. Don, High order weighted essentially non-oscillatory WENO-Z schemes for hyperbolic conservation laws, J. Comput. Phys. 230 (2011) 1766–1792.

[6] P. Chandrashekar and M. Zenk, Well-balanced nodal discontinuous Galerkin method for Euler equations with gravity, J. Sci. Comput. 71 (2015) 1062–1093.

[7] A. Chertock, S. Cui, A. Kurganovz, S.N. Özcan and E.Tadmor, Well-balanced central-upwind schemes for the Euler equations with gravitation, SIAM J. Sci. Comput. submitted.

[8] X. Deng, M. Mao, Y. Jiang and H. Liu, New high-order hybrid cell-edge and cell-node weighted compact nonlinear scheme. In: Proceedings of 20th AIAA CFD conference, AIAA 2011-3847, June 27-30, Honoluu, HI, USA, 2011.

[9] X. Deng and H. Maekawa, Compact high-order accurate nonlinear schemes, J. Comput. Phys. 130 (1997) 77–91.

[10] X. Deng and H. Zhang, Developing high-order weighted compact nonlinear schemes, J. Comput. Phys. 165 (2000) 22–44.

[11] V. Desveaux, M. Zenk, C. Berthon and C. Klingenberg, A well-balanced scheme for the Euler equation with a gravitational potential. Finite Vol. Complex Appl. VII-Methods Theor. Asp. Springer Proc. Math. Stat. 77 (2014) 217–226.

[12] Z. Gao and G.H. Hu, High order well-balanced weighted compact nonlinear schemes for the shallow water equations, Comm. Comput. Phys. Accepted.

[13] G.S. Jiang and C.-W. Shu, Efficient implementation of weighted ENO Schemes, J. Comput. Phys. 126 (1996) 202–228.

[14] R. Käppeli and S. Mishra, Well-balanced schemes for the euler equations with gravitation, J. Comput. Phys. 259 (2014) 199–219.

[15] S.A. Lele, Compact finite difference schemes with spectral-like resolution, J. Comput. Phys. 103(1) (1992) 16–42.

[16] R.J. LeVeque, Balancing source terms and flux gradients on high-resolution Godunov methods: the quasi-steady wave propagation algorithm, J. Comput. Phys. 146 (1998) 346–365.

[17] R.J. LeVeque, D.S. Bale, Wave propagation methods for conservation laws with source terms, In: Proceedings of the 7th International Conference on Hyperbolic Problems, (1998) 609–618.

[18] G. Li and Y.L. Xing, Well-balanced discontinuous Galerkin Methods for the Euler equations under gravitational fields, J. Sci. Comput. 67 (2016) 493–513.

[19] G. Li and Y.L. Xing, High order finite volume WENO schemes for the Euler equations under gravitational fields, J. Comput. Phys. 316 (2016) 145–163.

[20] G. Li, C.N. Lu and J.X. Qiu, Hybrid well-balanced WENO schemes with different indicators for shallow water equations, J. Sci. Comput. 51 (2012) 527–559.

[21] X.L. Liu, S.H. Zhang, H.X. Zhang and C.-W. Shu, A new class of central compact schemes with spectral-like resolution I: Linear schemes, J. Comput. Phys. 248 (2013) 235–256.

https://doi.org/10.4208/eajam.181016.300517g Published online by Cambridge University Press

[22] J. Luo, K. Xu and N. Liu, A well-balanced symplecticity-preserving gas-kinetic scheme for hydrodynamic equations under gravitational field, SIAM J. Sci. Comput. 33 (2011) 2356–2381.
[23] T. Nonomura and K. Fujii, Effects of difference scheme type in high-order weighted compact nonlinear schemes, J. Comput. Phys. 228 (2009) 3533–3539.
[24] T. Nonomura and K. Fujii, Robust explicit formulation of weighted compact nonlinear scheme, Comput. Fluids 85 (2013) 8–18.
[25] T. Nonomura, N. Iizuka and K. Fujii, Freestream and vortex preservation properties of high-order WENO and WCNS on curvilinear grids, Comput. Fluids 39(2) (2010) 197–214.
[26] T. Nonomura, N. Iizuka and K. Fujii, Increasing order of accuracy of weighted compact nonlinear scheme, In: AIAA-2007-893, 2007.
[27] B. Perthame and C. Simeoni, A kinetic scheme for the Saint-Venant system with a source term, Calcolo 38, (2001) 201–231.
[28] C.-W. Shu, Essentially non-oscillatory and weighted essentially non-oscillatory schemes for hyperbolic conservation laws, in: B. Cockburn, C. Johnson, C.-W. Shu, E. Tadmor (Ed.: A. Quarteroni) Advanced Numerical Approximation of Nonlinear Hyperbolic Equations, Lecture Notes in Mathematics, Springer, 1697 (1998) 325–432.
[29] C.-W. Shu and S. Osher, Efficient implementation of essentially non-oscillatory shock-capturing schemes, J. Comput. Phys. 77 (1988) 439–471.
[30] A. Slyz, K.H. Prendergast, Time independent gravitational fields in the BGK scheme for hydrodynamics, Astron. Astrophys. Suppl. Ser. 139 (1999) 199–217.
[31] C.T. Tian, K. Xu, K.L. Chan and L.C. Deng, A three-dimensional multidimensional gas-kinetic scheme for the Navier-Stokes equations under gravitational fields, J. Comput. Phys. 226 (2007) 2003–2027.
[32] Y. Xing and C.-W. Shu, A survey of high order schemes for the shallow water equations, J. Math. Study 47 (2014) 221–249.
[33] Y. Xing and C.-W. Shu, High order well-balanced WENO scheme for the gas dynamics equations under gravitational fields, J. Sci. Comput. 54 (2013) 645–662.
[34] Y. Xing and C.-W. Shu, High order finite difference WENO schemes with the exact conservation property for the shallow water equations, J. Comput. Phys. 208 (2005) 206–227.
[35] Y. Xing and C.-W. Shu, High order well-balanced finite difference WENO schemes for a class of hyperbolic systems with source terms, J. Sci. Comput. 27 (2006) 477–494.
[36] Y. Xing and X. Zhang, Positivity-preserving well-balanced discontinuous Galerkin methods for the shallow water equations on unstructured triangular meshes, J. Sci. Comput. 57 (2013) 19–41.
[37] K. Xu, A well-balanced gas-kinetic scheme for the shallow-water equations with source terms, J. Comput. Phys. 178 (2002) 533–562.
[38] S. Zhang, S. Jiang and C.-W. Shu, Development of nonlinear weighted compact schemes with increasingly higher order accuracy, J. Comput. Phys. 227 (2008) 7294–321.
[39] Q.Q. Zhu, Z. Gao, W.S. Don and X.Q. Lv, Well-balanced hybrid Compact-WENO Schemes for shallow water equations, Appl. Num. Math. 112 (2017) 65–78.

https://doi.org/10.4208/eajam.181016.300517g Published online by Cambridge University Press